Catal Lett (2008) 126:188–192
DOI 10.1007/s10562-008-9605-3

Effects of Modified Beta Zeolites with Acid on Anisole Acetylation in a Fixed Bed Reactor

Dishun Zhao · Jinlong Wang · Juan Zhang

Received: 17 June 2008 / Accepted: 27 July 2008 /

Abstract A beta zeolite sample (Si/Al = 30) was modified by citric acid, tartaric acid, and hydrochloric acid. The catalytic performances of these zeolite together with another beta zeolite (Si/Al = 12.5) were tested in the anisole acetylation in a fixed-bed configuration. The zeolites were characterized by powder X-ray diffraction, FT-IR of adsorbed pyridine, and temperature programmed desorption of ammonia. The ratios of Si/Al, the specific surface areas, and the pore sizes were also measured. The results showed that the most active and stable behavior was achieved on the HCl treated zeolite. The strong acid sites as many as possible but with an appropriate concentration and strength were needed in order to obtain an optimum activity and stability.

Keywords Beta zeolite · Modification · Anisole · Acetylation · Fixed bed reactor

1 Introduction

Friedel–Crafts acylation of aromatics is one of the most important synthetic reactions for the preparation of aromatic ketones, which are key intermediates in the production of pharmaceuticals, dyes, fragrances, and agrochemicals [1–3]. The conventional methods for production of aromatic ketones involve acid chlorides or anhydrides used as acylated agents and Lewis acids such as $AlCl_3$, BF_3 etc. used as catalysts. As a consequence, a number of problems including the need of more than stoichiometric amounts of catalysts with production of a large amounts of inorganic by-products, in particular hydrochloric acid, and the cumbersome work-up steps resulting from the hydrolysis of the mixtures of the products, are effected. Moreover, the Lewis acid catalysts cannot be regenerated [4–8].

In view of the disadvantages of the homogeneous Lewis acid catalysts in current practical aromatics acylation reactions, considerable efforts have been made to develop heterogeneous solid acid catalysts [9–13]. Zeolites, with their unique acid properties and pore structures, exhibit good catalytic activity and selectivity in the acylation of aromatic compounds [3, 14, 15].

However, zeolites as acylation catalysts often suffer from fast deactivation and often need regeneration. The reasons for the catalyst deactivation can be attributed to the dealumination of zeolites by the acidic byproducts and the stable adsorption of heavy products and the permanent deposition of carbonaceous substances on the active sites of the catalysts [16, 17]. Results showed that the stability of zeolites can be improved by increasing the molar ratio of the substrate aromatic ether [16], supporting zeolites on a preshaped carrier, e.g., SiC [2, 15, 18, 19], using the continuous fixed-bed configurations [16], and so on. The study of the effects of the modified zeolites with acids on the acylation of aromatics in a fixed bed reactor was scarcely seen.

In this paper, the effects of modified beta zeolites with acids on the activity and stability of anisole acetylation by acetic anhydrous with an equimolar ratio of ether to anhydride in a fixed bed reactor were studied. The beta zeolites before and after modification were characterized.

D. Zhao (✉) · J. Wang · J. Zhang
School of Chemical Engineering and Technology,
Tianjin University, Tianjin 300072, China
e-mail: dishunzhao@yahoo.com.cn

D. Zhao
College of Chemistry and Pharmaceutical Engineering,
Hebei University of Science and Technology,
Shijiazhuang 050018, China

An attempt was made to establish a correlation between the activity and stability on one hand and the properties of zeolite on the other hand in the acylation of anisole.

2 Experiment

2.1 Catalysts

A commercial NH_4-BEA (Si/Al = 12.5) was kindly provided by Research Institute of Petroleum Processing. The HBEA (labeled $\beta 1$) was obtained by calcinating the NH_4-BEA at 823 K for 6 h. Another kind of HBEA zeolite (Si/Al = 30, labeled $\beta 2$) was purchased from Nankai University Catalyst Co., Ltd.

Zeolite $\beta 2$ of 5 g was subjected to acid treatments by stirring with an approximate 0.7 mol L^{-1} citric acid, 0.5 mol L^{-1} tartaric acid at 353–363 K for 4 h, respectively. The resultant zeolites were washed with deionized water and dried at 393 K. After that the acid treated zeolites were calcinated at 823 K for 4 h. The prepared zeolites were labeled CA-$\beta 2$, TA-$\beta 2$, respectively.

Zeolite $\beta 2$ of 5 g was subjected to an acid treatment by stirring with an approximate 1.0 mol L^{-1} hydrochloric acid at room temperature for 1 h. The resultant zeolite was washed with deionized water and dried at 393 K. After that the acid treated zeolite was calcinated at 823 K for 4 h. The prepared sample was labeled HA-$\beta 2$.

2.2 Catalytic Tests

Zeolites $\beta 1$, $\beta 2$, CA-$\beta 2$, TA-$\beta 2$, HA-$\beta 2$ were pelletized and crushed in order to obtain particles within 0.4–1 mm in diameter. Before the catalytic tests, the same amount of zeolites was calcined at 823 K for 6 h. To avoid exposure to ambient atmosphere, the zeolites were transferred while hot into a glass reactor.

The catalytic tests were carried out in the fixed-bed configuration at 363–373 K under atmospheric pressure. The mixtures of anisole and acetic anhydrous with a molar ratio of 1:1 were fed into the reactor by a syringe pump with a given flow rate corresponding to a weight hourly space velocity of 13.3 h^{-1}.

Reaction samples were taken in regular intervals and analyzed by gas chromatography equipped with a PEG 20 M column, 30 m × 0.32 mm × 0.50 μm film thickness, biphenyl in 1,2-dichloroethane used as the internal standard solution.

After the first cycle, the catalysts were collected together and again activated at 823 K for 6 h followed by drying at 393 K. The catalytic behavior was re-tested under the same conditions. The tests were repeated for three times.

2.3 Characterization Techniques

X-ray diffraction patterns of the zeolites were recorded with a Rigaku D/MAX 2500 PC powder X-ray diffractometer operating at 40 kV and 80 mA, using the nickel filtered Cu-Kα radiation.

Energy dispersive X-ray spectroscopy (EDS) (EX 250) equipped on scanning electron microscope S4800-I, Hitachi, was employed for the determination of the ratios of Si/Al.

BET surface areas and pore size distribution were measured by recording the nitrogen adsorption/desorption isotherm at a liquid nitrogen temperature with the use of a Quantachrome Autosorb Automated Gas Sorption system. Before each measurement, the zeolites were evacuated in order to remove impurities on the surface.

The acidity of zeolites was determined by the pyridine adsorption–desorption method performing on a Bruker Vector 22 infrared spectrometric analyzer. A self-supported wafer of around 20 mg with a diameter of 16 mm was placed in an infrared cell connected to a vacuum system. Zeolites were evacuated at 673 K for 90 min in a vacuum. After the self-supported wafer was cooled down to ambient temperature, pyridine was adsorbed for 30 min and then the physisorption pyridine was evacuated at 473 K for 1.0 h. The IR spectra were obtained at 473 K.

Temperature programmed desorption (TPD) of NH_3 was carried out on TPDRO 1100 Series apparatus of Thermo Electron Corporation. NH_3 was adsorbed at room temperature for 1.0 h. The zeolites were measured with a heating rate of 40 K min^{-1}. Nitrogen with a flow rate of 20 mL min^{-1} was used as the carrier gas.

3 Results and Discussion

3.1 Structure and Composition

Figure 1 shows the X-ray diffraction patterns of zeolites $\beta 1$, $\beta 2$, CA-$\beta 2$, TA-$\beta 2$, and HA-$\beta 2$. It indicates that the acid treatment zeolites, CA-$\beta 2$, TA-$\beta 2$, and HA-$\beta 2$, had the BEA structure of $\beta 2$. The characteristic diffraction peaks of CA-$\beta 2$, TA-$\beta 2$, and HA-$\beta 2$ were all at 7.8° and 22.5° just like $\beta 1$ and $\beta 2$ and the five zeolites all possessed high crystallinity [20]. Acid treatments did not change the structure of beta zeolites, and there were no visible peaks from any impurities.

According to the results of EDS as illustrated in Table 1, the ratios of Si/Al were 36.5, 35.9, and 38.1 for the zeolites CA-$\beta 2$, TA-$\beta 2$, and HA-$\beta 2$, respectively.

3.2 Catalytic Activity and Stability

Acetylation of anisole by acetic anhydride with a molar ratio of 1:1 over a HBEA zeolite with a Si/Al ratio of 12.5

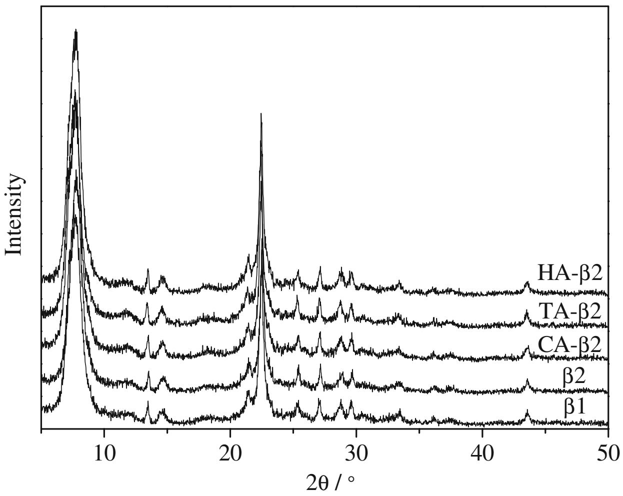

Fig. 1 XRD patterns of the five zeolites

Table 1 The ratios of Si/Al of the zeolites

Sample	*β*1	*β*2	CA-*β*2	TA-*β*2	HA-*β*2
Si/Al	12.5	30	36.5	35.9	38.1

in a fixed-bed configuration was reported by Rohan et al. [16]. The results they obtained were close to those of *β*1 in our paper (Fig. 2a). The difference was the initial activity probably due to the powder samples they used instead of granules of ours and the relatively slow flow rate. The low conversion of the beginning time on stream can be attributed to the activation period of the catalysts. Zeolite *β*2 gave a slightly higher conversion of anisole and was more stable than *β*1. After acid treatment, CA-*β*2 and TA-*β*2 had a similar activity and stability. Among the five zeolites, HA-*β*2 gave the highest conversion and was the most stable (Fig. 2b).

It first seems that the activity and stability were increased with the increase of the ratio of Si/Al without a linear connection. However, a further study on the HCl treated zeolites indicated that the activity and stability did not increase with the increase of the HCl concentration (not shown). As the ratio of Si/Al of modified zeolites increased because of dealumination by HCl, it suggested that other factors played more important role than the ratio of Si/Al.

It is well known that Friedel–Crafts acylation reaction on zeolites was catalyzed by the BrØnsted acid and the deactivation of the catalysts was due to the carbonaceous substances retaining in the micropores and mesopores [9, 10, 16]. So the acidity, specific surface areas, and pore diameters of the zeolites were measured in order to account for the above catalytic behavior.

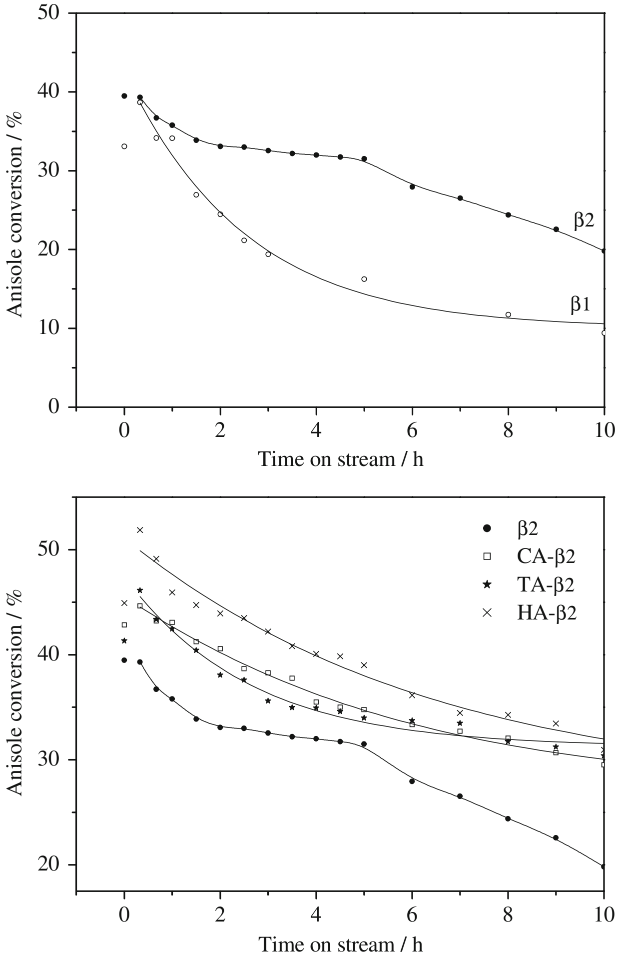

Fig. 2 Acylation of anisole at 363–373 K in a fixed bed reactor. (**a**) *β*2 versus *β*1, (**b**) CA-*β*2, TA-*β*2, HA-*β*2 versus *β*2

3.3 Specific Surface Areas and Pore Diameters

Table 2 illustrates the specific surface areas and pore diameters of the zeolites. Unmodified zeolites *β*1 and *β*2 had the similar specific surface area and the same pore diameter. However, the specific surface areas became larger and the diameters of the pores became smaller after acid treatments with CA-*β*2 having the largest specific surface area and TA-*β*2 having the smallest pore diameter.

3.4 Acid Sites

The information of Brønsted and Lewis acid sites can be gained by the FT-IR spectra of adsorbed pyridine in the region of 1,400–1,600 cm^{-1}. Bands near 1,540 cm^{-1} can be ascribed to pyridine molecules protonated on Brønsted acid sites whereas 1,450 cm^{-1} pyridine on Lewis acid sites. A reliable representation of the concentration of surface acid sites (mmol g^{-1}) can be the integrated peak areas [21].

Table 2 Physical properties and acid sites determined by pyridine-IR spectra for different samples

Sample	BET (m^2 g^{-1})	Pore diameter (nm) (SF method)	B acid site[a]	L acid site[a]
$\beta 1$	464	0.8721	1.21	5.28
$\beta 2$	457	0.8721	0.83	4.14
CA-$\beta 2$	507	0.8536	0.43	2.92
TA-$\beta 2$	484	0.8444	0.62	3.02
HA-$\beta 2$	487	0.8536	0.83	3.12

[a] Calculated by the ratio of the integrated area of IR adsorption peak to sample weight

Table 2 also illustrates the acid sites determined by pyridine-IR spectra for different samples. As expected, $\beta 2$ with the higher ratio of Si/Al possessed less amounts of Brønsted and Lewis acid sites. The acid modified zeolites had the same (HA-$\beta 2$) or less amounts (CA-$\beta 2$, TA-$\beta 2$) of Brønsted and Lewis acid sites.

3.5 Acid Strength Distribution

In the NH_3-TPD experiment, the amount of desorbed ammonia can be considered as the amount of the acid sites of the samples. The strength of the acid sites can be determined by the desorption temperature [22]. Table 3 gives the NH_3-TPD data for different zeolites and the NH_3-TPD profiles of the zeolites are shown in Fig. 3.

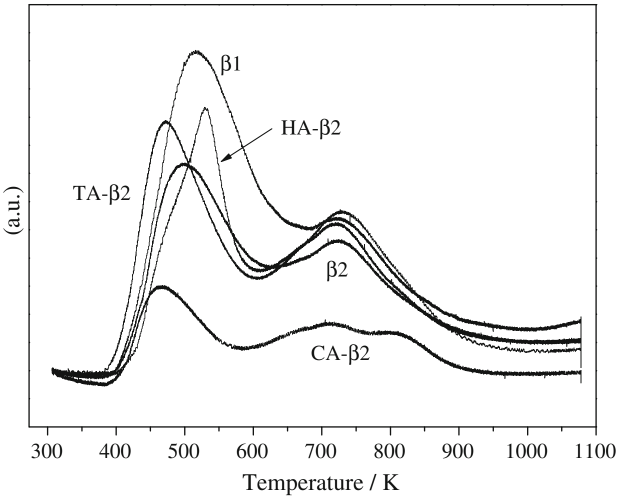

Fig. 3 NH_3-TPD profiles of the zeolites

Compared with $\beta 1$, there was a decrease in the weak acid amount and strength and the total acid amount but an increase in the strong acid amount and strength in $\beta 2$. Compared with $\beta 2$, tartaric acid treated zeolite TA-$\beta 2$ had a more decrease in the weak acid amount and strength but a slight increase in the strong acid amount and strength and the total acid amount. HCl treated zeolite HA-$\beta 2$ had a large increase in the weak acid strength but a slight decrease in the strong acid amount and strength. It is very interesting to note that the NH_3-TPD pattern of citric acid treated zeolite CA-$\beta 2$ possessed three peaks. Its low-temperature peak was much lower than that of $\beta 2$ and high-temperature peak was slightly lower than the high-temperature peak of $\beta 2$. Besides these, there was an existence of a super high-temperature peak near 783 K. But the corresponding acid amount was less.

It can be imagined that catalysts with large amounts of total acid sites do not necessarily exhibit a higher activity. Large amounts of acid sites with a higher acid strength may mean a higher activity but may deactivate faster. So an ideal catalyst with an optimum activity and stability may possess acid sites as many as possible but with an appropriate concentration and strength. This can explain the behaviors of the tested zeolites. Zeolite $\beta 2$ with a higher ratio of strong acid amount to weak acid amount was more active than zeolite $\beta 1$. TA-$\beta 2$ and HA-$\beta 2$ had an even higher ratio of strong acid amount to weak acid amount but had a larger specific surface area than zeolite $\beta 2$, so both were more active and stable than zeolite $\beta 2$. Moreover, the pore diameter of TA-$\beta 2$ was 0.028 nm smaller than zeolite $\beta 2$, which was an important factor preventing carbonaceous materials from depositing on its surface. Although

Table 3 NH_3-TPD data for different samples

Sample	T peak (K)		Acid amount, n (NH_3) (mmol g^{-1})			
	L T-peak[a]	H T-peak[b]	Total acid	Weak acid	Strong acid	Strong acid/weak acid
$\beta 1$	516	713	0.84	0.62	0.22	0.35
$\beta 2$	496	724	0.55	0.32	0.23	0.72
CA-$\beta 2$	471	711/783	0.23	0.11	0.08/0.04	
TA-$\beta 2$	472	728	0.57	0.30	0.28	0.93
HA-$\beta 2$	529	720	0.43	0.22	0.21	0.95

[a] L T-peak: low-temperature peak

[b] H T-peak: high-temperature peak

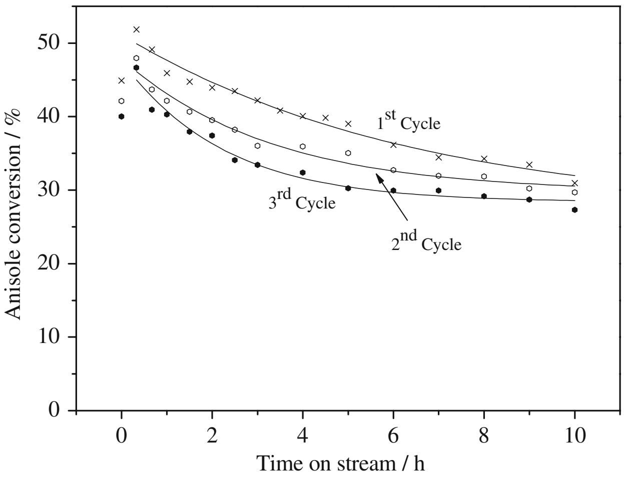

Fig. 4 Acetylation of anisole on the HCl treated zeolite, HA-β2

there were much fewer acid sites in CA-β2, it had a fraction of most strong acid amount and the largest specific surface area. So CA-β2 was an active and stable catalyst, too.

3.6 Regeneration of the Catalyst

Figure 4 shows the results of the acetylation of anisole on HA-β2 during three cycles. It indicates that the activity and stability of the catalyst can be satisfactorily recovered, which meant that most of the acid sites can be restored to its initial states.

4 Conclusion

The effects of modified beta zeolites with citric acid, tartaric acid, and hydrochloric acid on the activity and stability of anisole acetylation in a fixed bed reactor were studied. The results showed that the HCl treated zeolite exhibit the most active and stable behavior. The beta zeolites before and after modification were characterized. It indicated that in order to increase the activity and also slow the deactivation, an optimum acidity should be obtained so that the strong acid sites were as many as possible but with an appropriate concentration and strength. The hydrophobic or crystallite size of the zeolites was probably also effective, but it was beyond the subject investigated here.

References

1. Smith K, Zhao ZhH, Hodgson PKG (1998) J Mol Catal 134:121
2. Winé G, Matta J, Tessonnier JP, Pham-Huu C, Ledoux MJ (2003) Chem Commun 4:530
3. Kantam ML, Ranganath KVS, Sateesh M, Kumar KBS, Choudary BM (2005) J Mol Catal A 225:15
4. Spagnol M, Gilbert L, Benazzi E, Marcilly C (1996) US Patent, WO9635656
5. Gaare K, Akporiaye D (1996) J Mol Catal A 109:177
6. Beers AEW, Hoek I, Nijhuis TA, Downing RS, Kapteijn F, Moulijn JA (2000) Top Catal 13:275
7. Alvaro M, Corma A, Das D, Fornés V, García H (2005) J Catal 231:48
8. Sartori G, Maggi R (2006) Chem Rev 106:1077
9. Freese U, Heinrich F, Roessner F (1999) Catal Today 49:237
10. Derouane EG, Dillon CJ, Bethell D, Derouane-Abd Hamid SB (1999) J Catal 187:209
11. Kaur J, Kozhevnikov IV (2002) Chem Commun 21:2508
12. Devassy BM, Halligudi SB, Hegde SG, Halger AB, Lefebvre F (2002) Chem Commun 10:1074
13. Bachiller-Baeza B, Anderson JA (2004) J Catal 228:225
14. Derouane EG, Crehan G, Dillon CJ, Bethell D, He H, Hamid SBDA (2000) J Catal 194:410
15. Winé G, Pham-Huu C, Ledoux MJ (2006) Catal Commun 7:768
16. Rohan D, Canaff C, Fromentin E, Guisnet M (1998) J Catal 177:296
17. Ji XF, Qin ZhF, Wang GF, Dong M, Hou XL, Wang JG (2006) J Chem Eng Data 51:1156
18. Winé G, Tessonnier JP, Pham-Huu C, Ledoux MJ (2002) Chem Commun 20:2418
19. Winé G, Tessonnier JP, Rigolet S, Marichal C, Ledoux MJ, Pham-Huu C (2006) J Mol Catal A 248:113
20. Ji XF, Qin ZhF, Dong M, Wang GF, Dou T, Wang JG (2007) Catal Lett 117:171
21. Xie ZK, Chen QK, Zhang ChF, Bao JQ, Cao YH (2000) J Phys Chem B 104:2853
22. Lenarda M, Ros MD, Casagrande M, Storaro L, Ganzerla R (2003) Inorg Chim Acta 349:195